



Numerical prediction of pressure loss of fluid in a T-junction

Mohammed Abdulwahhab¹, Niranjan Kumar Injeti¹, Sadoun Fahad Dakhil²

¹ Department of Marine Engineering, Andhra University, AP, India.

² Department of Fuel & Energy, Basrah Technical College, Iraq.

Abstract

This work presents a prediction of pressure loss of fluid with turbulent incompressible flow through a 90° tee junction was carried out and compared with analytical and experimental results. One turbulence model was used in the numerical simulations: k- ϵ model for two different values of area ratio between the main pipe and the branch pipe were 1.0 and 4.0, and flow rate ratios. The continuity, momentum and energy equations were discretized by means of a finite volume technique and the SIMPLE algorithm scheme was applied to link the pressure and velocity fields inside the domain. A three dimensional steady state flow was solving by using CFX 5 code ANSYS FLUENT13. The effect of the flow rate ratio q (ratio between the flow rate in the branch and outlet pipes) on pressure drop and velocity profile was predicted at different Reynolds numbers. The results show that increasing the flow rate ratio the pressure and total energy losses increase because the presence of recirculation and the strong streamline curvature. *Copyright © 2013 International Energy and Environment Foundation - All rights reserved.*

Keywords: T-junction; Pressure loss coefficient; Flow rate ratio.

1. Introduction

In this developing world the fluid is being transported through pipe lines for several kilo meters. For Eg: 90–95% of natural gas in U.S. is transported through 411,000 km of pipeline. The proposed Iran Pakistan India pipeline or the Peace pipeline is 2,775 KM long. Similarly millions of tons of crude oil are being transported from deep sea to on shore. In the lift irrigation system water is being transported to several thousands of kilometers. Under these circumstances there is a dire necessity to find out the pressure loss that take place during the flow process at micro level.

Analyzing the flow field in the vicinity of a single perforation can help to understanding the impact of inflow on the pressure drop in a perforated horizontal wellbore. Inflow entering the wellbore through a perforation and merging with wellbore flow in the well is considered similar to combining flow at a pipe junction. However, a large difference in flow rate and dimensions exists between these two cases. An area ratio, which is the cross sectional area of the branch pipe to that of the main pipe, and the flow rate ratio of branch pipe flow rate over main pipe flow rate have been used as two primary parameters to quantify the pressure loss of pipe junction flow. However, the area ratio of a perforation wellbore is normally much smaller than that of pipe junctions. Furthermore, a branch pipe can join the main pipe at different angles between the axis of the two pipes.

$$\Delta P_m = \frac{1}{2} \rho (u_3^2 - u_1^2) - \rho \frac{A_2}{A_3} u_2^2 \cos \theta \quad (2)$$

Defining the pressure loss coefficient in the main flow [7]

$$k_m = \frac{\Delta P_m}{0.5 \rho u_3^2} \quad (3)$$

where

$$q = \frac{Q_2}{Q_3} \quad (4)$$

$$k_m = 2q - \left(1 + 2 \frac{A_2}{A_3} \cos \theta\right) q^2 \quad (5)$$

Two empirical correlations are developed by [8]. The equations have the same form with different coefficients. The coefficients of one correlation are determined by least square method for all the series of tests comprising the given junction angles and area ratios. Finally the pressure loss coefficient is

$$k_m = 2.777 \frac{Q_2}{Q_3} - 2.151 \left(\frac{Q_2}{Q_3}\right)^2 \quad (6)$$

2.2 Governing equations

The equations to be solved for incompressible flow are the conservation of mass Eq. (6) and momentum Eq. (7) in Cartesian coordinate.

$$\frac{\partial U_i}{\partial x_i} = 0 \quad (7)$$

$$\frac{\partial \rho U_i}{\partial t} + \frac{\partial \rho U_j U_i}{\partial x_j} = -\frac{\partial \bar{p}}{\partial x_i} + \frac{\partial}{\partial x_j} \left[\mu \left(\frac{\partial U_i}{\partial x_j} + \frac{\partial U_j}{\partial x_i} \right) - \overline{\partial \rho u_i u_j} \right] \quad (8)$$

The above two equations (7) and (8) are the Navier-Stokes equations. Many researchers have attempted to solve these equations but the computational complexity involved has not allowed many but arrived at some solutions. Navier-Stokes equation can be solved numerically by using finite volume method, but the solutions are obtained only after making some assumptions and some of them are not stable at high Reynolds number.

The $k - \varepsilon$ model is one of the most commonly used turbulence models. It includes two transport equations to represent the turbulent properties of the flow. The first transported variable is turbulent kinetic energy. The second transported variable in this case is the turbulent dissipation ε . These variables determine the scale of the turbulence and energy in the turbulence. The $k - \varepsilon$ model is most commonly used to describe the behavior of the turbulent flow. $\overline{\partial \rho u_i u_j}$ represent the last term of equation (8) as a time average eddy shear stress in the momentum equation, where the molecular diffusion shear stress $\mu \frac{\partial u}{\partial x_i}$ is augmented by this shear stress and important role played in turbulent flow. Initially the $k - \varepsilon$ model was proposed by A.N. Kolmogorov in 1942, then further refined by Harlow and Nakayama and

finally proposed the $k - \varepsilon$ model for the fully turbulence flow. The Transport equations for $k - \varepsilon$ model are for [9]

$$\frac{\partial}{\partial t}(\rho k) + \frac{\partial}{\partial x_i}(\rho k u_i) = \frac{\partial}{\partial x_j} \left[\left(\mu + \frac{\mu_t}{\sigma_k} \right) \frac{\partial k}{\partial x_j} \right] + p_k + p_b - \rho \varepsilon - Y_k + S_k \quad (9)$$

And for ε ,

$$\frac{\partial}{\partial t}(\rho \varepsilon) + \frac{\partial}{\partial x_i}(\rho \varepsilon u_i) = \frac{\partial}{\partial x_j} \left[\left(\mu + \frac{\mu_t}{\sigma_\varepsilon} \right) \frac{\partial \varepsilon}{\partial x_j} \right] + C_{1\varepsilon} \frac{\varepsilon}{k} (P_k + C_{3\varepsilon} P_b) - C_{2\varepsilon} \rho \frac{\varepsilon^2}{k} + S_\varepsilon \quad (10)$$

Realizable k -epsilon model and RNG k -epsilon model are some other variation of k -epsilon model. k -epsilon model has solution in some special cases. k -epsilon model is only useful in regions with turbulent, high Reynolds number flows. The equations contain four adjustable constants. The standard $k - \varepsilon$ model employs values for the constants that are arrived at by comprehensive data fitting for a wide range of turbulent flows:

σ_k	σ_ε	$C_{1\varepsilon}$	$C_{2\varepsilon}$
1.00	1.30	1.44	1.92

3. Flow parameters

3.1 Flow geometry

The T-junction was drawn with the Cartesian coordinate system and the notation is presented in Figure 1. From Figure 1 the author has assumed that the diameter at inlet 1 and outlet 3 as x and the length between $5D$ and $3d$ as $2x$. Similarly the length between $2D$ and $0D$ as $2x$.

X is considered as one inch (0.0254 m), and the direction of main flow is Z direction as mentioned in the diagram. The origin of the coordinate system is located at the center of the pipe at entrance i.e. inlet 1. The T-piece looks very similar and with sharp edges.

3.2 Simulation parameters

The fluid used in the simulations is water with constant density of 998.2 kg/m^3 and dynamic viscosity of 0.001 kg/m s . The fluid is assumed as Incompressible flow. The boundary conditions were set as a mass flow at the two inlets and as pressure at the outlet. The two inlets depend on the value of velocities and the flow rate ratio between the inlet 2 and outlet 3. The inlet boundary conditions are normal to surface area of inlet 1 and inlet 2. The velocity at the inlet pipe (upstream) is fully developed. It is assumed that no-slip boundary conditions at all the walls. As the flow is axsymmetric the complete geometry is taken into consideration. Figure 2 is the unstructured computational grids (Tetrahedral cells), the mesh consist from 285568 nodes and 1098887 elements with five boundary layers. The calculations were carried out with commercial finite volume code CFX 5 using a second order scheme.

4. CFD simulation and results

From the computed pressure field, the longitudinal variation of pressure was processed to yield the local loss coefficients k_m referring to the flow from the inlet 1 to the outlet 3 in the main pipe according to the equations (2),(4), and (5) [7]. Computation of the pressure drop between inlet 1 and inlet 3 i.e. upstream and downstream of the main pipe is carried over with help of equation (2).

4.1 Loss coefficients

Interesting phenomena is observed that the pressure drop is caused by the presence of a T-piece. This is expressed by the non-dimensional coefficients defined in equation (3).

Figure 3 compares the values of pressure loss coefficient between analytical [7], experimental results. The present work is carried out by building a model making use of ICEM CFD with five boundary layers for the area ratio A_3/A_2 which is equal to one and the chosen angle $\theta = 90^\circ$.

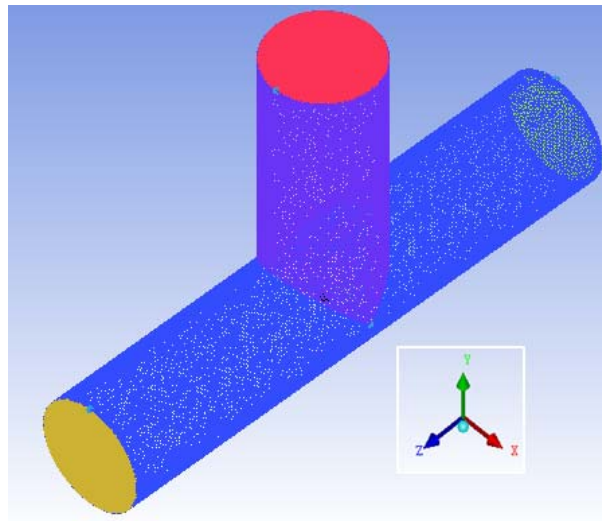


Figure 2. The unstructured mesh for T-junction

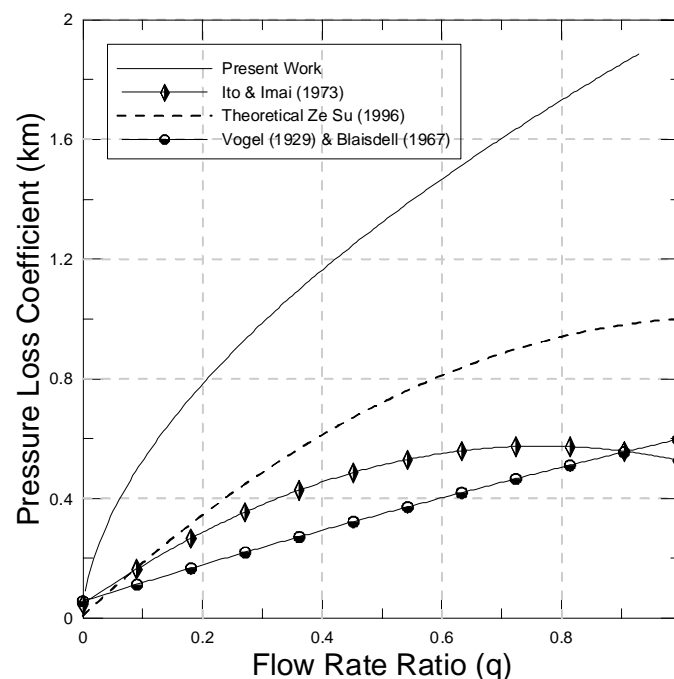


Figure 3. Pressure loss coefficients for combining flow $A_3/A_2=1.0$, $\theta = 90^\circ$

Experimental results obtained by [4-6] are very close and are demonstrated lower pressure loss coefficients than that given by the theoretical [7] when the flow rate ratio is higher than 0.1. Interestingly the results from the present work are higher than the theoretical values of previous researchers [7]. The reason is predicted that the previous researchers have not considered the forces applied on the main stream and the duct wall in the direction of the main pipe. From the results it is concluded that the pressure loss coefficient did not noticeably vary with the velocity of flow. This is an indication that the Reynolds number does not affect the pressure loss coefficient.

The tests in this research are carried out for branch pipe, which is of equal diameter as the main pipe and the area ratio $A_3/A_2 = 4$ joining the main pipe with angle $\theta = 90^\circ$.

The comparison of the shape of CFX profile with the analytic data reveals few differences. It shows that when the flow rate ratio increase is more than 0.2. Because at higher values of flow rate ratio the non-fully –developed flow occurs and creating a cavity near T-junction causing pressure drop. In other words as the velocity increases at the inlet 2, accordingly the pressure drop is taking place near T-Junction as shown in Figures 4 and 5.

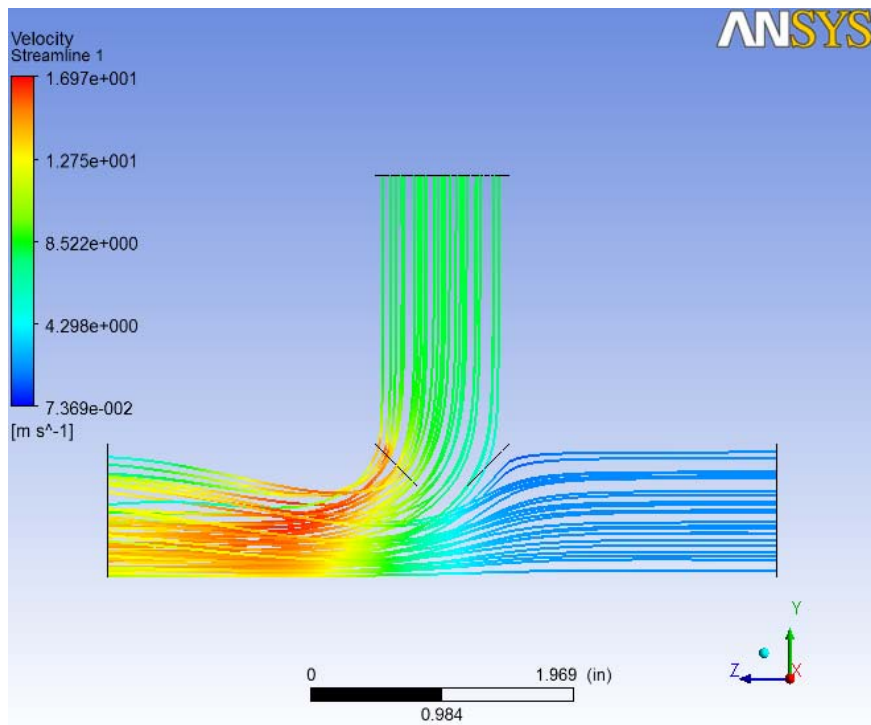


Figure 4. Streamline of velocity ($V_1 < V_2$), $A_3/A_2=1.0$, at $Re=50718$

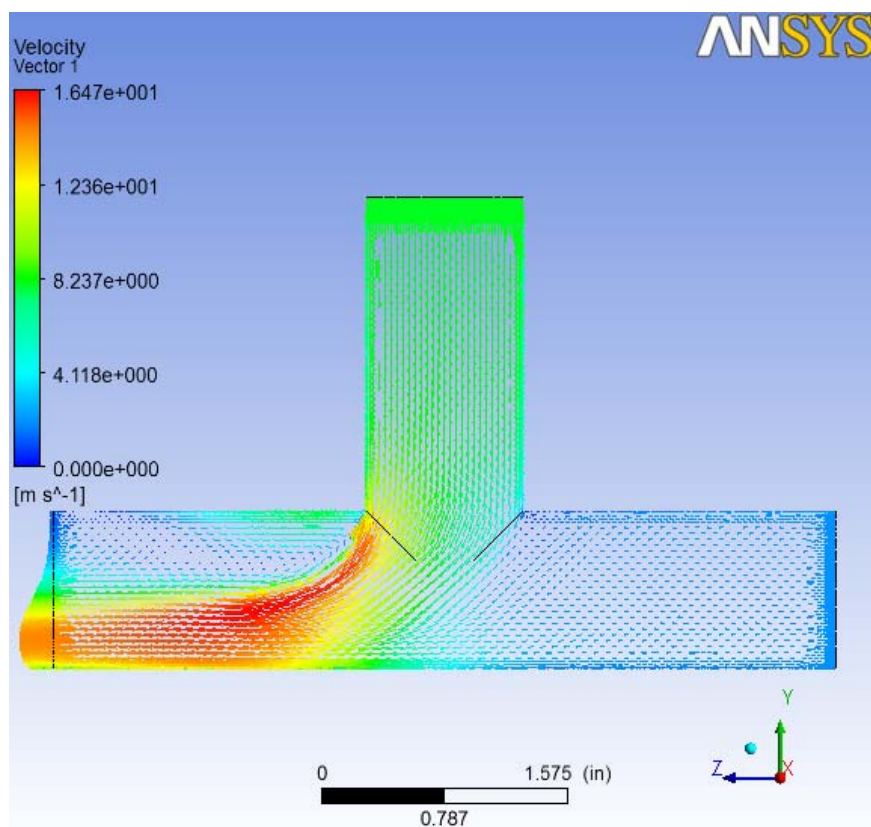


Figure 5. Vector of velocity ($V_1 < V_2$), $A_3/A_2=1.0$, at $Re=50718$

The junction energy loss coefficients in the main pipe agreed well among all the test results. The energy loss at the branch was represented by the mechanical potential drop Δe . Assuming the flow is incompressible, mechanical potential at any cross section along a passage was defined as the total pressure (kinetic energy and pressure energy).

The potential drop normalized by the square of the velocity as ordinate and the flow rate ratio as abscissa Figure 6. There is a difference of the curve shape of analytical [7] and experimental curve by [6]. The performance of CFX numerical curve of the author is in agreement with the experimental data with a slight difference with lower values of flow rate ratio which is less than 0.1. A more recent work was conducted at the institute of High Speed Mechanics in Tohoku University [4]. Only the energy losses caused by the combination of flow at smooth tees with diameter ratio as unity were studied.

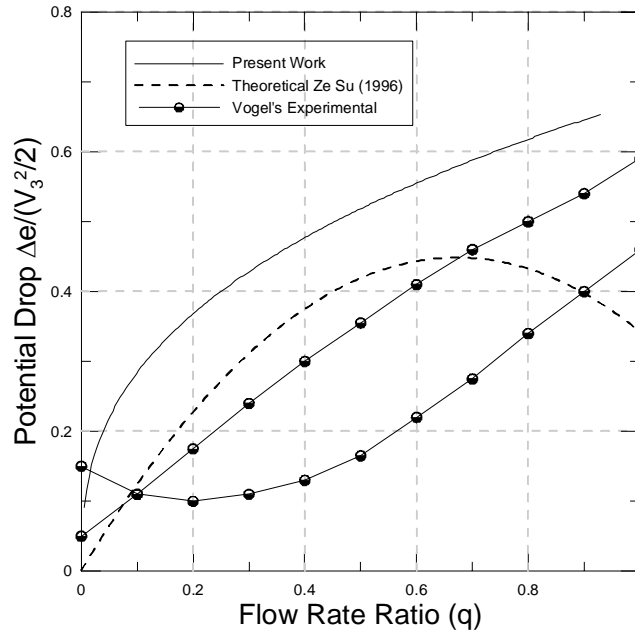


Figure 6. Energy drop for combining flow $A_3/A_2 = 1.0$, $\theta = 90^\circ$

The theoretical equation [7] does not include the effect of the curvature radius of the joining edge. Most experiments were conducted on sharp-edged junctions. The correlations obtained by [4, 10] were only based on the pipe diameter ratio is one and $\theta = 90^\circ$ angle between the main pipe and the branch. The data plotted as the function between pressure loss coefficient versus flow rate ratio shown in Figure 7 represents the data for the geometry of sharp-edged and 90° junction and unit pipe area ratio. The pressure loss coefficient in the main pipe is strongly affected by the geometry of the pipe junction.

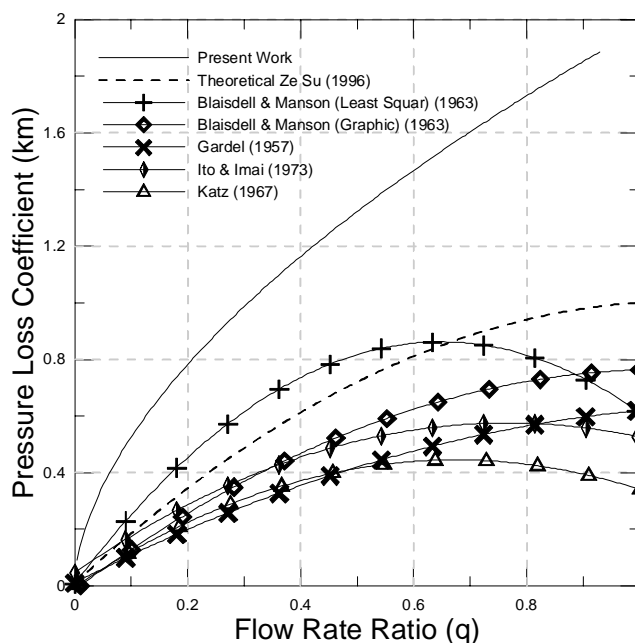


Figure 7. Comparison of CFX, theoretical, empirical and experimental data, $A1/A2=1$, $\theta = 90^\circ$

Figure 7 depicts that Lower values of Pressure loss coefficients than the data obtained from CFX analysis and it is observed that the shape of the curve is the same as that of the curve for the theoretical lower values. The difference between theoretical and CFX values increases with the increase of flow rate ratio ($q=Q_2/Q_3$) because in the theoretical data the wall shear stress is ignored and also ignored any force applied on the main and branch pipes.

Pressure loss coefficients are calculated for a sharp-edged and 90° T-junction with pipe area ratio A_3/A_2 is 4 by using numerical and compare it with theoretical equation and empirical correlations. They are plotted as a function of flow rate ratio in Figure 8.

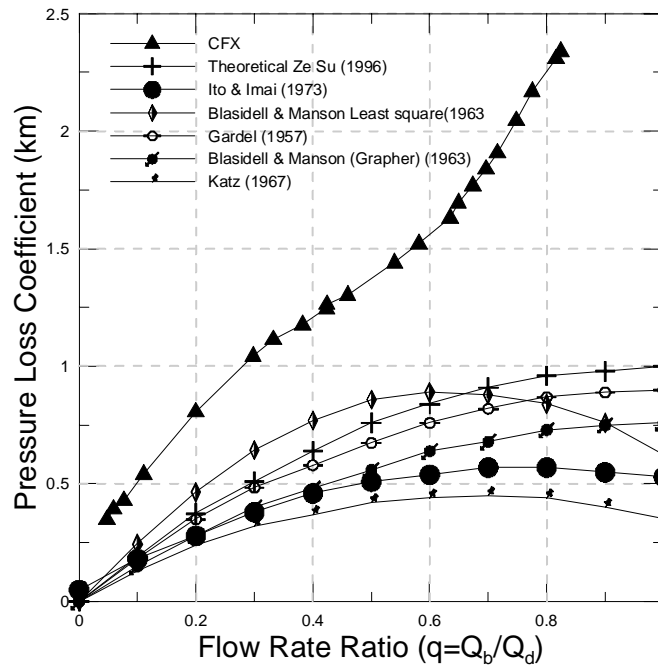


Figure 8. Comparison of numerical, theoretical, empirical and experimental data, $A_3/A_2=4.0$, $\theta = 90^\circ$

The values calculated by [2] correlation moved higher compared with that of unit pipe area ratio as shown in Figure 7. The values obtained from the theoretical equation and other correlations are remain unchanged, since the multiplication of area ratio and $\cos 90^\circ$ is zero. Experimental data obtained from researchers for pipe area ratio 1 and 4 are the same values under the same flow rate ratio, but with Gardel correlations for higher values compared with that of unit pipe area ratio. The results from ANSYS FLUENT 13 changed the shape of the curve after the value 0.4 for flow rate ratio (q). It is because of the fact that it depends on the value of inlet 2 velocity i.e. branch velocity. Increased value of velocity is noticed at inlet 2 and the dispersed stream lines are observed at the middle pipe. The generation of eddies and effect of swirl on the flow around a sphere or cylinder is also noticed. These eddies absorb a great deal of energy due their rotational kinetic energy and increased in pressure drop and therefore the loss coefficient is large.

Figure 9 depicts that streamlines generated between 0D and 2D at the inlet 1 is gradually moved towards the wall from the junction between 3D and 5D due to increased flow velocity of Inlet 2. It results to decrease in pressure ratio towards outlet 3.

Figure 10 shows the velocity vector for the above case and depicts higher velocity of the branch pipe than the main pipe at T-junction which results in drop in pressure.

Where from Figures 11 and 12 shows that there less pressure loss towards outlet. It is because of the fact that the velocities V_1 and V_2 of inlet 1 and inlet 2 are same.

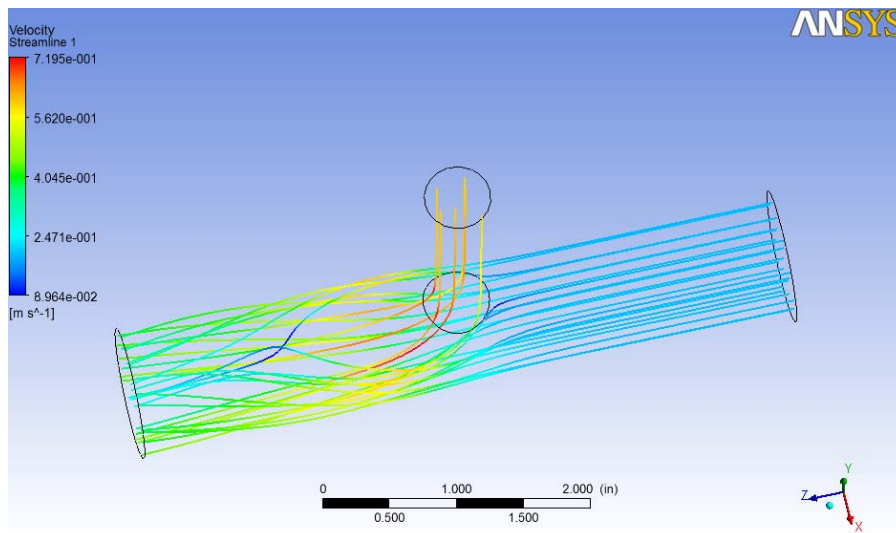


Figure 9. Streamlines of velocity ($V_2 > V_1$), $Re=5068$

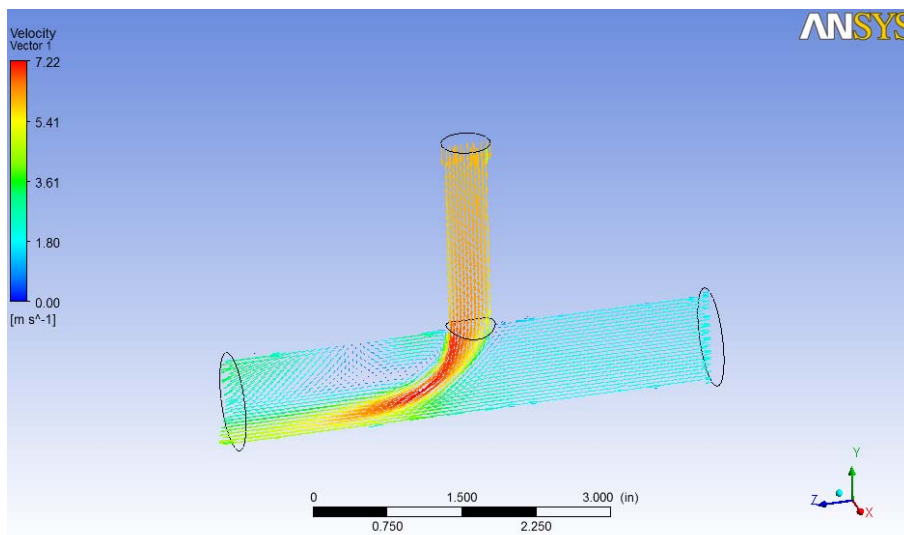


Figure 10. Velocity vector ($V_2 > V_1$), $Re=50676$

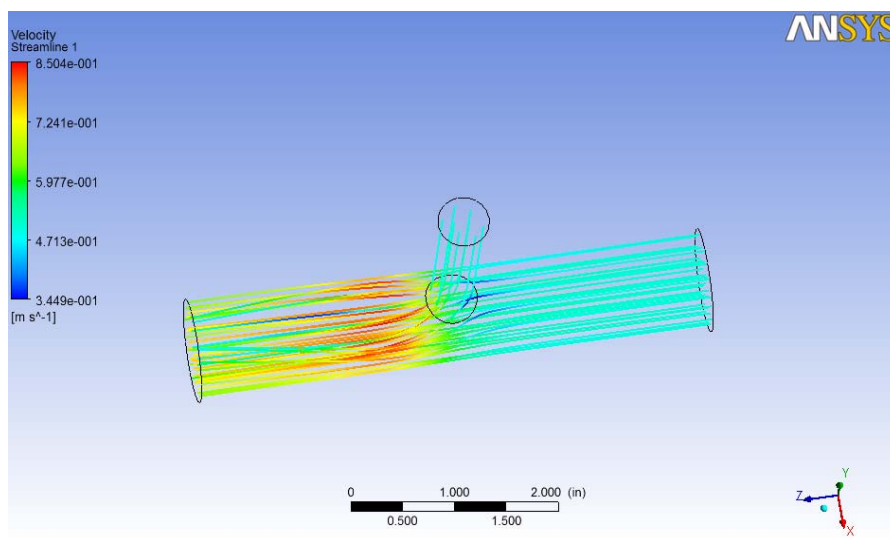


Figure 11. Streamlines of velocity ($V_1 = V_2$), $Re=12670$

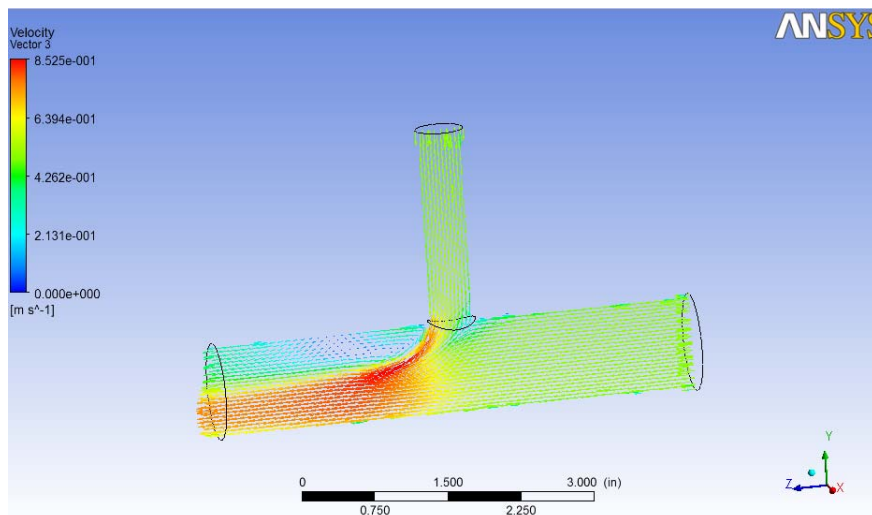


Figure 12. Velocity vector ($V_1=V_2$), $Re=12670$

4.2 Downstream of the T-Junction

Between 3D and 5D the author has assumed certain values from the center of the junction such as $z=3.25, 3.75, 4.25$ and 4.75 in inches of distance to study the velocity profile at various cross sections of the downstream pipe is depicted in Figure 13. The flow is the axial velocity i.e. Z direction. The axial mean velocity at inlet 1 is 1 m/s and inlet 2 it is 1.307 m/s . The profile of the velocities are different at different distances at downstream of the main pipe. The velocities at the line $z=3.25$ inches close to the branch are showing higher values at the center of pipe and gradually decreased towards the sides of the pipe. It is further observed that the lower value ($3.42e-01\text{ m/s}$) at $Y=0.3$ inches and from there after the velocity is gradually increased. The profile of the velocities at a distance $z=3.75$ inches are moving away towards the outlet which is different from the cross section where $z=3.25$ in. It is because the values higher than from previous position $z=3.25$ and the lower value occurred at $Y=0.2$ inches i.e. 0.645 m/s and then increased towards the upper side of the pipe. The profile of velocities at cross section $z=4.25$ in reveals few differences except at $Y=0.3$ inches where the values of velocities became lower. The deflection of the profile velocities at cross section $z=4.75$ inches, the shape of the curve depicts non-fully developed flow because the length of downstream is not sufficient to reach the fully developed.

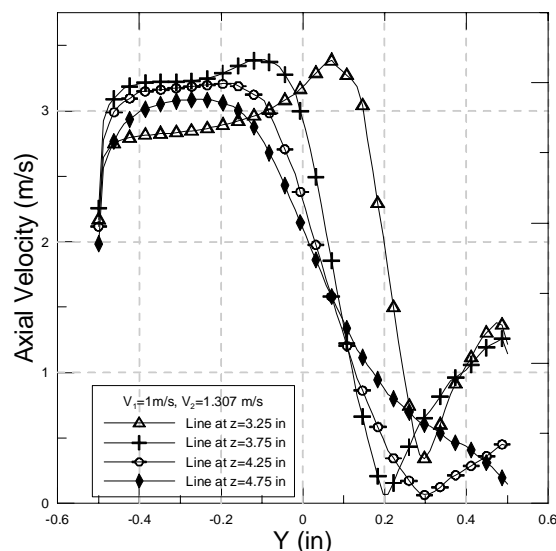


Figure 13. Comparison of axial velocities at $V_1=1\text{ m/s}$, $V_2=1.307\text{ m/s}$ at downstream of the main pipe

Figure 14 shows the profile of velocities at the branch pipe in $-y$ direction at different planes of cross section taken into consideration where $y=2, 1.5, 1.0, 0.50$ inches. It shows that the velocity profiles at cross sections $y=2$ inches and $y=1.5$ inches are observed the same behavior. It is because these lines lie

far away from the midpoint of T-junction and hence the profile is fully developed flow. The cross section at $y=1$ inches shows the shape of the inlet profile reveals a few differences with the previous cross sections. The cross section at $y=0.5$ inches directly with the zone connection of T-junction so the profile is fully different because this zone is affected by non-fully developed flow.

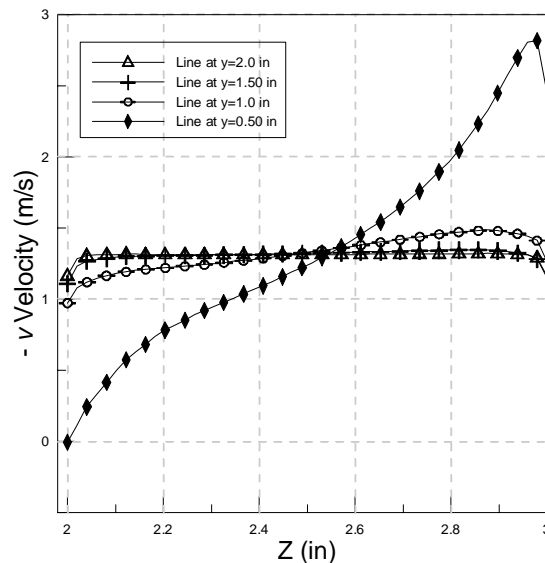


Figure 14. Comparison of axial velocities at $V_2=1.307$ m/s at branch pipe

5. Conclusions

Predictions of the turbulent flow in a 90° T-Junction were carried out and compared with theoretical and experimental data for two cases as the pipe area ratio $A_3/A_2=1.0$ and 4.0 for sharp edged. The pressure loss coefficient given by the numerical results is higher than those obtained from theoretical and experimental results. The higher the flow rate ratio is the higher the difference between them. The behavior of the curve of pressure loss coefficient for pipe area ratio 1.0 is different from curve for pipe area ratio 4.0 especially after the flow rate ratio $q=0.4$ because the value of velocity at inlet 2 is greater than the velocity at inlet 1 and this causes the recirculation of the downstream fluid of the main pipe.

Acknowledgment

To all the people who helped me, thank you. Prof. Niranjana Kumar and Ass. Prof. Sadoun Fahad your patience, guidance and support aided me in countless ways allowing me to complete this work. I appreciate Prof. T.V.K. Bhanuprakash provided numerous answers to my countless questions.

Nomenclature

A_1 [m ²]	main pipe area at inlet 1	A_2 [m ²]	branch pipe area
A_3	[m ²] main pipe area at outlet	$C_{1\epsilon}, C_{2\epsilon}, C_k$	Standard k-epsilon model constants
CFD	Computational Fluid Dynamic	D_1 [m]	main pipe diameter
D_2	branch pipe diameter	k [m ² /s ²]	turbulent kinetic energy
k_m	pressure loss coefficient	L [m]	length of pipe
P_1 [pa]	pressure at inlet1	P_2 [pa]	pressure at inlet2 (branch pipe)
P_3 [pa]	pressure at outlet3	P_b	effect of buoyancy
P_k	production of k	ΔP_m [pa]	pressure difference
q	flow rate ratio	Q_1 [m ³ /s]	flow rate at inlet
Q_2 [m ³ /s]	flow rate at branch	Q_3 [m ³ /s]	flow rate at outlet
Re	Reynolds number	S	modulus of the mean rate of strain tensor
t [s]	time	u_1 [m/s]	velocity at inlet1
u_2 [m/s]	velocity at branch (inlet2)	u_3 [m/s]	velocity at outlet
\bar{u} [m/s]	x-component of mean velocity	u_i [m/s]	velocity (fluct. i th comp.)
U [m/s]	velocity (mean x-component)	V [m/s]	axial velocity

Greek conventions

μ [kg/ms]	dynamic viscosity	μ_t [kg/ms]	turbulent viscosity
ρ [kg/m ³]	density	k [m ² /s ²]	turbulent kinetic energy
ε [m ² /s ³]	turbulent dissipation rate	σ_k	turbulent Prandtl number for k
σ_ε	turbulent Prandtl number for ε	θ	angle between main and branch pipes

Subscripts

i, j i_{th}, j_{th} coordinate, pipe identifier

References

- [1] Smeeta Fokeer, Ph. D. (2006), "An Investigation of Geometrically Induced Swirl Applied To Lean Phase Pneumatic Flows".
- [2] Gardel, A., (1957) "Les pertes de charge dans les écoulements au Travers de branchements en Te", Bulletin Technique de la Suisse Romande, Nr. 9 & 10.
- [3] Maia, R. J., 1992, "Numerical and experimental investigations of the local losses in piping systems. Methods and Techniques for its systematic investigation. The specific case of the flow in a 90° Tee junction" PhD thesis, University of Porto, Portugal (in Portuguese).
- [4] Ito, H. and Imai, K., "Energy Loss at 90° Pipe Junctions." Proc. ASCE, Journal of Hydraulics Division, September 1973, pp. 1353-1968.
- [5] Blaisdell, F. W. and Manson, P. W. (1967), "Energy Loss at Pipe Junctions," Proc. ASCE, Journal of the Irrigation and Drainage Division, September, 93 (IR3), pp. 59-78.
- [6] Vogel, G., (1929) "Experiments to Determine the Loss at Right Angle Pipe Tees," Hydraulic laboratory practice (ed. Freeman, J.R.), pp. 470-472, Published by American Society of Mechanical Engineers.
- [7] Ze Su, (1996) "Pressure Drop in Perforated Pipes for Horizontal Wells". Ph. D., Norwegian.
- [8] Blaisdell, F. W. and Manson, P. W. (1963), "Loss of Energy at sharp -Edged Pipe Junctions in Water Conveyance systems", Agricultural Research Service, U.S. Department of Agricultural and Minnesota Agricultural Experiment Station, St. Anthony Falls Hydraulic Lab., U of Minnesota.
- [9] Paritosh R. Vasava, (2007), "Fluid Flow in T-Junction of Pipes". Ms. C. thesis, Lappeenranta University of Technology.
- [10] Katz, S., "Mechanical Potential Drops at a Fluid Branch," Journal of Basic Engineering Trans. ASME, December, 1967, Vol. 89, pp. 732-36.



Mohammed Abdulwahhab Marine Engineer, Arab Gulf Academy, B.Sc. 1986, Master of Science in Mechanical Engineering, Basrah University, Iraq 1996. Ph.D. research scholar, Marine Engineering, Andhra University, India from September 2011 till now. Major Field of study: Fluid Flow, Energy, Horizontal oil wells.
E-mail address: mohw2002@yahoo.com



Niranjan Kumar Injeti Mechanical Production Engineering, B. E. Andhra University, Visakhapatnam, India June 1986. M. E., Cryogenic Engineering, Indian Institute of Technology, Kharagpur, WB, India, 1987. Ph. D. Marine Engineering (Marine Turbo Machinery lab) Andhra University, 2004. Major Field: Fluid Flow, Stress Analysis, Heat Transfer, Combustion, life Evaluation of Critical Components of Gas Turbine. Professor Dr. Injeti has 4 papers published at International journals, 12 International conferences and 2 National conferences.
E-mail address: neeru9@yahoo.com, neerux@yahoo.com



Sadoun Fahad Dakhil Sadoun Fahad Dakhil, Mechanical Engineer, University of Technological, 1980 Baghdad-Iraq. M. Sc. Thermal Engineering, Basrah University, Iraq 1991. Ph. D. Thermal Engineering, Basrah University, Iraq 2007. Major Field: Heat Transfer, Internal Combustion Engine, Fluid Flow, Horizontal Oil Wells. He has 1 paper published at International journal, 8 National Journals and 6 National conferences.
E-mail address: sadoun_fahad_55@yahoo.com